Self-Assembly of α-Helical Polypeptides Driven by Complex Coacervation

*Dimitrios Priftis, Lorraine Leon, Ziyuan Song, Sarah L. Perry, Khatcher O. Margossian, Anna Tropnikova, Jianjun Cheng, and Matthew Tirrell**

Abstract: Reported is the ability of α-helical polypeptides to self-assemble with oppositely-charged polypeptides to form liquid complexes while maintaining their α-helical secondary structure. Coupling the α-helical polypeptide to a neutral, hydrophilic polymer and subsequent complexation enables the formation of nanoscale coacervate-core micelles. While previous reports on polypeptide complexation demonstrated a critical dependence of the nature of the complex (liquid versus solid) on chirality, the α-helical structure of the positively charged polypeptide prevents the formation of β-sheets, which would otherwise drive the assembly into a solid state, thereby, enabling coacervate formation between two chiral components. The higher charge density of the assembly, a result of the folding of the α-helical polypeptide, provides enhanced resistance to salts known to inhibit polypeptide complexation. The unique combination of properties of these materials can enhance the known potential of fluid polypeptide complexes for delivery of biologically relevant molecules.

Complexation of oppositely charged polyelectrolytes in aqueous media can lead to liquid–liquid phase equilibria, referred to as complex coacervation, which is driven by a combination of entropic and enthalpic effects.[1–3] A variety of polyelectrolytes have been utilized in coacervation, ranging from bio-macromolecules such as gum Arabic or chitosan,[4,5] to proteins such as lysozyme and β-lactoglobulin,[6,7] to synthetic polymers such as poly(ethylene imine) or poly-(acrylic acid)[8–10] and polypeptides.[11] This communication introduces complex coacervation in a new class of materials which possess unusual helical stability against changing environmental conditions and maintain strong electrostatic interactions. The design principle for these polypeptide-based materials was the extension of the hydrophobic side chains bearing a positively charged terminal amine group. When the charged groups are moved away from the peptide backbone (minimum of 11 σ-bonds) the overall charge on the helical

surface is reduced, thus allowing the polypeptides to simultaneously maintain water solubility and helical stability.[12] The goal of this work is to investigate the self-assembly of this type of material and analogous diblock copolymers with oppositely charged homo-polypeptides. The effects of polypeptide chirality, salt concentration, and polymer chain length on the resultant self-assembly structures are evaluated.

Because of the interesting interfacial and bulk-material properties (e.g., low interfacial energy with water),[13,14] complex coacervates have found applications in the pharmaceutical and food industries as encapsulants, as well as underwater adhesives.[15–19] In addition to bulk coacervate materials, the use of molecular architecture strategies, such as block copolymers which link polyelectrolyte domains to a neutral, hydrophilic polymer enables microphase separation, or self-assembly, on the nanometer scale. A variety of self-assembled structures such as coacervate core micelles or hydrogels have been reported with the use of this strategy.[20–24] An advantageous feature of these assemblies is the sensitivity of the coacervate domains to a number of parameters (e.g., pH, salt, concentration, polymer length) and it conveniently allows control of the assembly and the mechanical properties of the self-assembled structures. Furthermore, the coacervate cores of these assemblies can serve as nanoreservoirs for various charged or hydrophilic compounds (e.g., DNA, RNA), thus allowing control of the encapsulation and properties such as stability, solubility, and reactivity.[25,26]

Recently, we demonstrated that charged polypeptides can undergo complex coacervation and studied how this phenomenon is affected by a number of parameters (e.g., pH, salt, mixing ratio).[11] Polypeptides represent an interesting class of materials because of their potential biocompatibility, ability to incorporate bioactive epitopes and secondary structural motifs (e.g., α-helix), and sequence specificity. Charged polypeptides, such as poly(lysine), adopt a random coil conformation at physiological pH as a result of side-chain charge repulsion. Upon neutralization of the charges at high pH, these polypeptides can form α-helices in much the same way as naturally hydrophobic polypeptides such as poly-(alanine).[27,28] However, the usefulness of poly(alanine) for generating secondary structure is limited because of the need for high pH and/or poor aqueous solubility. Furthermore, while previous research has shown that complex coacervates can be formed from polypeptides[11] recent experiments revealed that the nature (i.e., solid or liquid) of the complexes depends on the polypeptide chirality.[29] Fourier transform infrared (FTIR) spectroscopy and CD spectroscopy showed that when homochiral polypeptides are mixed (L-L, D-D or

[*] Dr. D. Priftis, Dr. L. Leon, Dr. S. L. Perry, K. O. Margossian,
A. Tropnikova, Prof. M. Tirrell
Institute for Molecular Engineering, University of Chicago
Chicago, IL 60637 (USA)
E-mail: mtirrell@uchicago.edu

Z. Song, Prof. J. Cheng
Department of Materials Science and Engineering, University of Illinois at Urbana-Champaign
Urbana, IL 61801 (USA)

Supporting information for this article is available on the WWW under http://dx.doi.org/10.1002/anie.201504861.

L-D) solid complexes with characteristics of aggregated β-strands are formed, whereas incorporation of at least one racemic polypeptide results in the formation of random coil, liquid complexes. The formation of coacervates correlates with the prevention of the formation of β-strands by the racemic polypeptide.

Herein we test the ability of specially designed polypeptides and diblock co-polypeptides, with stable α-helical structures, to self-assemble with oppositely charged homopolypeptides, assembly which results in fluid complexes (Scheme 1). The potential of this class of helical polypeptides
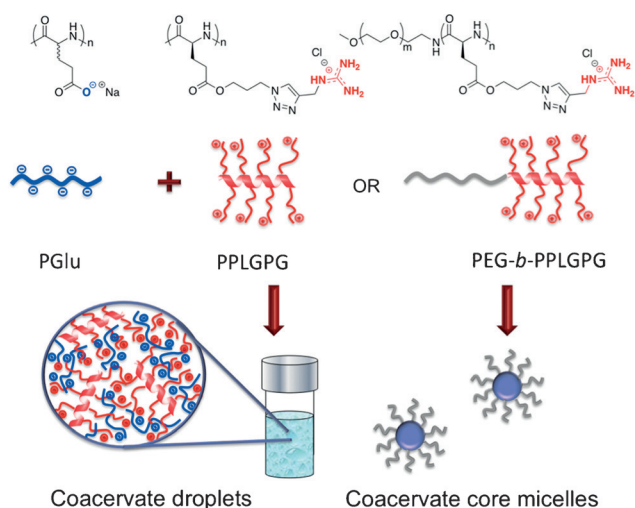

Scheme 1. Schematic representation of the self-assembly of α-helical homo- or co-polypeptides by complex coacervation.

has been demonstrated for gene delivery, and could easily be extended beyond DNA-peptide complexes to include other charged or water-soluble therapeutics by taking advantage of encapsulation in a coacervate-based matrix.[30–32] Unless otherwise stated for this study, racemic poly(glutamic acid) (PGlu) and poly(ethylene glycol)-*b*-poly(glutamic acid) (PEG-*b*-PGlu) were used as the polyanions while the α-helical polypeptide poly(γ-3-(4-(guanidinomethyl)-1*H*-1,2,3-triazol-1-yl)propyl-L-glutamate (PPLGPG) and diblock co-polypeptide poly(ethylene glycol)-*b*-polypeptide (PEG-*b*-PPLGPG) were used as the polycations. Poly(L-lysine) (PLys) was used as a polycation with random coil structure.

Synthesis of the α-helical PPLGPG polypeptides was achieved by ring-opening polymerization of the chlorine-based amino acid *N*-carboxyanhydride with subsequent side-chain end functionalization (see Figure S1 in the Supporting Information).[33] Similar to earlier studies,[20,21] the use of a PGlu precursor for the preparation of PPLGPG allows the synthesis of symmetric polymers with a well-defined mass. A similar procedure was used to synthesize PEG-*b*-(PPLGPG) co-polypeptides (see Figure S2 in the Supporting Information). The successful synthesis was confirmed with ^{1}H NMR spectroscopy (see Figure S3 in the Supporting Information) while the α-helical character of the synthesized polypeptides at pH 7.0 was verified by circular dichroism (CD; see Figure S4 in the Supporting Information). Samples were

prepared by mixing aqueous solutions of a polyanion and a polycation at a charged-matched stoichiometry, typically in the presence of salt (for experimental details see the methods section in the Supporting Information). Complexation between the oppositely charged polypeptides resulted in the formation of micrometer-scale liquid droplets (complex coacervates), as verified by optical microscopy (Figure 1B and Figure S5 in the Supporting Information).
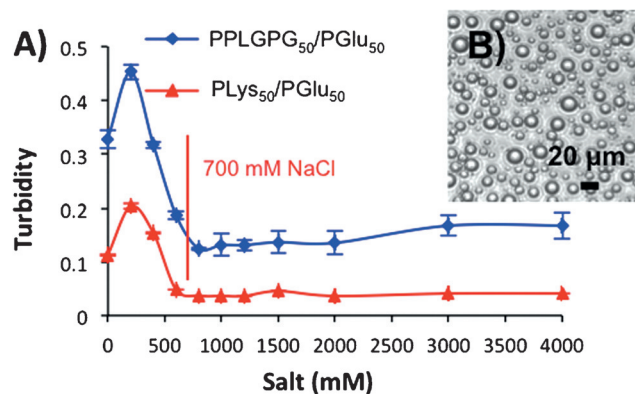

Figure 1. A) Turbidity indicating complex formation as a function of salt concentration for PPLGPG$_{50}$/PGlu$_{50}$ and PLys$_{50}$/PGlu$_{50}$. B) Optical microscopy image of PPLGPG$_{50}$/PGlu$_{50}$ coacervate droplets formed at 4.0 M NaCl (1 mM total polymer concentration in polymer, 1:1 mixing ratio, pH 7.0).

The polyelectrolyte mixing experiments described in the previous paragraph revealed that the dependence of the liquid or solid nature of the formed complexes on the chirality of the initial components vanishes when helical polypeptides such as PPLGPG are used. Direct observation by optical microscopy verified the formation of liquid coacervates from the complexation of PPLGPG with either homochiral (L or D) or racemic (R) poly(glutamic acid) (Figure 1B and Figure S5A–S5C). The liquid nature of the polypeptide complexes was also verified through rheology. The rheological response of a polypeptide complex, formed from chiral PPLGPG$_{50}$ and PGlu$_{50}$ polypeptides (the subscripts represent the number of repeating units or the molecular weight of polypeptides and PEG, respectively), to an oscillatory strain is described in Figure S6 in the Supporting Information. Frequency sweeps showed behavior similar to a viscoelastic liquid, and is consistent with previous rheological characterization of complex coacervates formed with at least one racemic polyelectrolyte.[8,34,35] This ability to form liquid complexes, regardless of the chirality of the partnering polypeptide, derives from the prevention of the formation of β-strands, which leads to solid complexes when only chiral polypeptides are used.[29]

The effect of salt on polypeptide complex formation was studied by turbidity. Comparative results from PPLGPG$_{50}$/PGlu$_{50}$ and PLys$_{50}$/PGlu$_{50}$ complexes are presented in Figure 1A. Consistent with previous coacervate studies,[8,9,26] complex formation was enhanced at low salt concentrations, followed by a steady decrease with increasing salt concentration. For PLys$_{50}$/PGlu$_{50}$, a characteristic critical salt con-

centration was observed at 0.7 M NaCl, above which phase separation no longer occurs and turbidity values equal those of aqueous solution. Surprisingly, we were unable to observe such a critical salt concentration for the PPLGPG$_{50}$/PGlu$_{50}$ system (up to a concentration of 4.0 M NaCl, the highest concentration tested). The unexpectedly high resistance to dissolution by salt can be related to the higher charge density of the α-helical PPLGPG (from chain folding), compared to random coil PLys, as predicted by theoretical and experimental studies.[36,37]

In addition to the formation of bulk complex coacervates by macrophase separation, microphase separation can be achieved by tethering the polyelectrolyte domain to a neutral polymer, such as PEG, thus resulting in the formation of nanometer-scale coacervate core micelles (Scheme 1).[38–40] The complexation of PEG$_{10k}$-b-PPLGPG$_{50}$ with PGlu$_{100}$ in dilute solution was initially investigated using dynamic light scattering (DLS). Mixing of the solutions under salt-free conditions and a charge-matched stoichiometry led to the formation of spherical micelles with a hydrodynamic diameter of approximately 36 nm (Figure 2 A and Table S2 in the Supporting Information). The shape and size measured through DLS was confirmed by negative-stain transmission electron microscopy (TEM; Figure 2 B). Small-angle X-ray
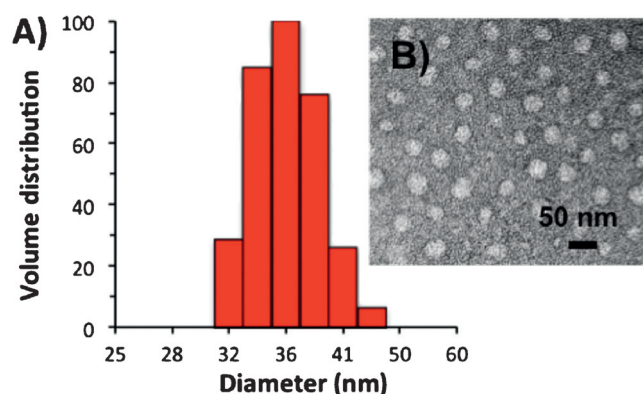

Figure 2. Characterization of coacervate core micelles. A) DLS histogram and B) negative-stain TEM image of PEG$_{10k}$-b-PPLGPG$_{50}$/PGlu$_{100}$ micelles (1 mM total polymer concentration in polymer, 1:1 mixing ratio, pH 7.0, 0 salt).

scattering (SAXS) measurements provided confirmation of the shape and size of the micelles. Fitting of the data using a core–shell form factor for spherical particles in dilute solutions[41] (see Figure S7 in the Supporting Information) gave excellent agreement between SAXS and DLS data (overall micelle diameter of 36 nm with both techniques). Similar self-assembled structures (see Figure S8C in the Supporting Information) were formed from mixing PEG$_{5k}$-b-PGlu$_{50}$ and PPLGPG$_{50}$ solutions, thus indicating that the type (i.e., negatively or positively charged) of polymer attached to the neutral block is not of importance.

Previous studies on coacervate core micelles utilizing random coil polypeptides showed that the size of the micelle was determined by the length of the PEG and polypeptide segments of the block copolymer, and not by the length of the

complexing homopolymer.[42] The modular nature of our synthetic approach allowed us to confirm the influence of polymer chain length in a micellar system involving α-helical polypeptides. Complexing PEG$_{10k}$-b-PPLGPG$_{50}$ with both PGlu$_{50}$ and PGlu$_{100}$ at a charge-matched mixing ratio, we observed no significant change in micelle size (diameters of 35.1 nm versus 35.7 nm were determined by DLS; see Table S2 in the Supporting Information). However, on increasing the length of the PEG block, we observed a significant increase in size of the self-assembled structure (35.7 nm and 47.9 nm for PEG 10k and 20k, respectively; see Table S2). This size increase correlated with results from TEM (Figure S7) and SAXS (36 nm and 44 nm, respectively; see Figure S8).

Micellar complexes also enabled analysis of the α-helical character of the polypeptide chain conformation within the coacervate core of the micelles using CD. Upon complexation, the PPLGPG polypeptides in the micelle core retained their α-helical conformations, as indicated by the characteristic double minima in the spectrum at $\lambda = 208$ and 222 nm (Figure 3). The calculated apparent helicity was similar among micelles formed with PEG$_{10k}$-b-PPLGPG$_{50}$ and
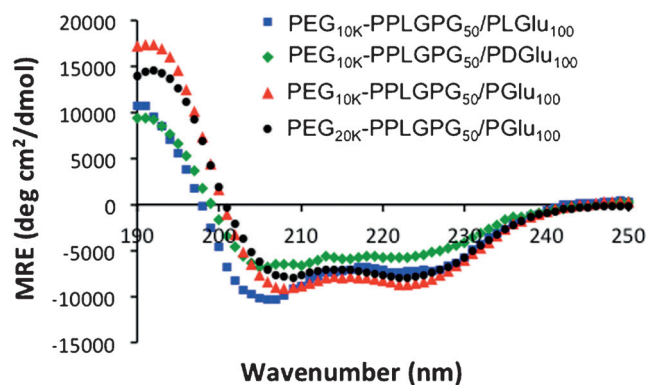
Figure 3. CD spectra of coacervate core micelles showing the effects of chirality (A) and PEG length (B; 0.25 mM total polymer concentration in polymer, 1:1 mixing ratio, pH 7.0, 0 salt).

chiral P(L)Glu$_{100}$ or P(D)Glu$_{100}$ (64 and 56%, respectively) and was higher (92%) when racemic PGlu$_{100}$ was used. This variation is related to the contributions to the spectrum from the homochiral (L or D) PGlu, as compared to the racemic PGlu, which effectively contributes no signal. Upon increasing the length of the PEG chain (from 10k to 20k), we also observed a reduction in the apparent helicity of micelles from 92 to 78%, thus suggesting that an increase in the PEG chain length affects the helix-forming ability of the PPLGPG polypeptides within the confined geometry of the micelle.

As with bulk complex coacervates, coacervate core micelles formed from a variety of polyelectrolytes respond to changes in the ionic strength.[43] We utilized DLS and TEM imaging to track variations in micelle size as a function of salt concentration (0–4.0 M of NaCl; see Tables S2 and S3). Remarkably, the size of the micelles formed with α-helical polypeptides showed very little variation over the entire range of salt concentrations. This data suggests that there is no

salt-induced morphological change in the self-assembled structure. Furthermore, we were unable to observe a critical salt concentration where the polyelectrolyte complex micelles dissociate completely, as in the case of the bulk materials.[24,44,45] As mentioned previously, the high stability of these complexes with respect to salt is caused by the high charge density of the α-helical conformation of the PPLGPG in the coacervate core, thus providing enhanced resistance compared to complexes formed from traditional random coil, charged polypeptides.[11]

In summary, we have demonstrated the ability of specially designed α-helical polypeptides to self-assemble with oppositely charged, random coil polypeptides to form structures that exhibit unique characteristics, as compared to those of typical polyelectrolyte complexes. First of all, the α-helical structure of the polypeptide prevents the formation of β-strands, which would otherwise drive the assembly into a solid state. This structure allows the formation of liquid complexes, even between two chiral components, which in the case of bulk-phase materials is advantageous for encapsulation of biomolecules.[46] Furthermore, the α-helical structure of the positively charged polypeptide is maintained in the coacervate core. Finally, the increased charge density of the α-helical structure provides enhanced stability to the assembled structure with respect to salt, and can be challenging at physiological conditions when small-molecular-weight polymers are used. Self-assembled complexes (i.e., micelles) formed from polypeptides have shown outstanding features as drug nanocarriers and on several occasions have proceeded to clinical trials.[47] The self-assembled structures described here show enhanced stability, α-helicity, and fluidity compared to other polypeptide systems, and could increase the potential of polypeptide-based complex coacervates in drug or gene delivery applications.

Experimental Section

Details of α-helical polypeptide synthesis and subsequent characterization, descriptions of methods, optical micrographs of complex coacervates, negative-stain TEM images of coacervate core micelles, CD analysis of various α-helical polypeptides, DLS data, and details of the fitting results used for the characterization of SAXS data are described in detail in the Supporting Information.

Acknowledgements

[1] D. Priftis, N. Laugel, M. Tirrell, *Langmuir* **2012**, *28*, 15947.
[2] C. B. Bucur, Z. Sui, J. B. Schlenoff, *J. Am. Chem. Soc.* **2006**, *128*, 13690.
[3] P. M. Biesheuvel, M. A. Cohen Stuart, *Langmuir* **2004**, *20*, 2785.
[4] B. Chloé, F. Salaün, *Carbohydr. Polym.* **2014**, *99*, 608.
[5] Y. J. Oh, I. H. Cho, H. Lee, K. J. Park, H. Lee, *Chem. Commun.* **2012**, *48*, 11895.
[6] S. Lindhoud, L. Voorhaar, R. de Vries, R. Schweins, M. A. C. Stuart, W. Norde, *Langmuir* **2009**, *25*, 6.
[7] F. Weinbreck, R. de Vries, P. Schrooyen, C. G. de Kruif, *Biomacromolecules* **2003**, *4*, 293.
[8] D. Priftis, K. Megley, N. Laugel, M. Tirrell, *J. Colloid Interface Sci.* **2013**, *398*, 39.
[9] R. Chollakup, W. Smitthipong, C. D. Eisenbach, M. Tirrell, *Macromolecules* **2010**, *43*, 2518.
[10] S. Perry, Y. Li, D. Priftis, L. Leon, M. Tirrell, *Polymer* **2014**, *6*, 1756.
[11] D. Priftis, M. Tirrell, *Soft Matter* **2012**, *8*, 9396.
[12] H. Lu, Y. Wang, Y. Bai, J. W. Lang, Y. Lin, J. Cheng, *Nat. Commun.* **2011**, *2*, 206.
[13] D. Priftis, R. Farina, M. Tirrell, *Langmuir* **2012**, *28*, 8721.
[14] E. Spruijt, J. Sprakel, M. A. Cohen Stuart, J. van der Gucht, *Soft Matter* **2009**, *6*, 172.
[15] H. Chu, J. Gao, C. W. Chen, J. Huard, Y. Wang, *Proc. Natl. Acad. Sci. USA* **2011**, *108*, 33.
[16] S. R. Bhatia, S. F. Khattak, S. C. Roberts, *Curr. Opin. Colloid Interface Sci.* **2005**, *10*, 45.
[17] H. Zhao, C. Sun, R. J. Stewart, J. H. Waite, *J. Biol. Chem.* **2005**, *280*, 42938.
[18] R. J. Stewart, *J. Exp. Biol.* **2004**, *207*, 4727.
[19] F. Weinbreck, H. Nieuwenhuijse, G. W. Robijn, C. G. de Kruif, *J. Agric. Food Chem.* **2004**, *52*, 3550.
[20] J. N. Hunt, K. E. Feldman, N. A. Lynd, J. Deek, L. M. Campos, J. M. Spruell, B. M. Hernandez, E. J. Kramer, C. J. Hawker, *Adv. Mater.* **2011**, *23*, 2327.
[21] D. V. Krogstad, N. A. Lynd, S. H. Choi, J. M. Spruell, C. J. Hawker, E. J. Kramer, M. Tirrell, *Macromolecules* **2013**, *46*, 1512.
[22] M. Lemmers, J. Sprakel, I. K. Voets, J. van der Gucht, M. A. Cohen Stuart, *Angew. Chem. Int. Ed.* **2010**, *49*, 708; *Angew. Chem.* **2010**, *122*, 720.
[23] R. P. Johnson, Y. I. Jeong, J. V. John, C. W. Chung, D. H. Kang, M. Selvaraj, H. Suh, I. Kim, *Biomacromolecules* **2013**, *14*, 1434.
[24] J. S. Park, Y. Akiyama, Y. Yamasaki, K. Kataoka, *Langmuir* **2007**, *23*, 138.
[25] Y. Kakizawa, K. Kataoka, *Adv. Drug Delivery Rev.* **2002**, *54*, 203.
[26] C. H. Kuo, L. Leon, E. J. Chung, R. T. Huang, T. J. Sontag, C. A. Reardon, G. S. Getz, M. Tirrell, Y. Fang, *J. Mater. Chem. B* **2014**, *2*, 8142.
[27] C. Dobson, A. Sali, M. Karplus, *Angew. Chem. Int. Ed.* **1998**, *37*, 868; *Angew. Chem.* **1998**, *110*, 908.
[28] A. Chakrabartty, T. Kortemme, R. Baldwin, *Protein Sci.* **1994**, *3*, 843.
[29] S. Perry, L. Leon, K. Hoffmann, M. Kade, D. Priftis, D. Wong, R. Klein, C. Pierce, K. Margossian, J. Whitmer, J. Qin, J. de Pablo, M. Tirrell, *Nat. Commun.* **2015**, *6*, 6052.
[30] L. Yin, H. Tang, K. H. Kim, N. Zheng, Z. Song, N. P. Gabrielson, H. Lu, J. Cheng, *Angew. Chem. Int. Ed.* **2013**, *52*, 9182; *Angew. Chem.* **2013**, *125*, 9352.
[31] N. P. Gabrielson, H. Lu, L. Yin, D. Li, F. Wang, J. Cheng, *Angew. Chem. Int. Ed.* **2012**, *51*, 1143; *Angew. Chem.* **2012**, *124*, 1169.

[32] R. Zhang, N. Zheng, Z. Song, L. Yin, J. Cheng, *Biomaterials* **2014**, *35*, 3443.

[33] H. Tang, L. Yin, K. H. Kim, J. Cheng, *Chem. Sci.* **2013**, *4*, 3839.

[34] R. Liu, Y. Morishima, F. Winnik, *Polym. J.* **2002**, *34*, 340.

[35] E. Spruijt, J. Sprakel, M. Lemmers, M. Stuart, J. van der Gucht, *Phys. Rev. Lett.* **2010**, *105*, 208301.

[36] D. Priftis, X. Xia, K. Margossian, S. Perry, L. Leon, J. Qin, J. de Pablo, M. Tirrell, *Macromolecules* **2014**, *47*, 3076.

[37] J. Overbeek, M. Voorn, *J. Cell. Physiol. Suppl.* **1957**, *49*, 7.

[38] A. Harada, K. Kataoka, *Macromolecules* **1995**, *28*, 5294.

[39] A. Kabanov, T. Bronich, V. Kabanov, K. Yu, A. Eisenberg, *Macromolecules* **1996**, *29*, 6797.

[40] J. F. Gohy, S. K. Varshney, S. Antoun, R. Jérôme, *Macromolecules* **2000**, *33*, 9298.

[41] J. Ilavsky, P. R. Jemian, *J. Appl. Crystallogr.* **2009**, *42*, 347.

[42] A. Harada, K. Kataoka, *Macromolecules* **2003**, *36*, 4995.

[43] I. K. Voets, A. de Keizer, M. C. Stuart, *Adv. Colloid Interface Sci.* **2009**, *147*, 300.

[44] S. V. Solomatin, T. K. Bronich, A. Eisenberg, V. Kabanov, A. Kabanov, *Langmuir* **2004**, *20*, 2066.

[45] K. Nakai, M. Nishiuchi, M. Inoue, K. Ishihara, Y. Sanada, K. Sakurai, S. I. Yusa, *Langmuir* **2013**, *29*, 9651.

[46] K. Black, D. Priftis, S. Perry, J. Yip, W. Byun, M. Tirrell, *ACS Macro Lett.* **2014**, *3*, 1088.

[47] H. Cabral, K. Kataoka, *J. Controlled Release* **2014**, *190*, 465.